Reconstructing three-dimensional oil palm architecture from allometric relationships

R. Perez[1,2], B. Pallas[2], S. Griffon[1], H. Rey[1], J.P. Caliman[3], G. Le Moguédec[4], J. Dauzat[1] and E. Costes[2]

[1]CIRAD, UMR AMAP, 34398 Montpellier Cedex 5, France; [2]INRA, UMR 1334 AGAP, 34398 Montpellier Cedex 5, France; [3]SMART Research Institute, Pekanbaru 28112, Indonesia; [4]INRA, UMR AMAP, 34398 Montpellier Cedex 5, France.

Abstract

The development of new breeding strategies to find more sustainable and productive systems is a major challenge to cope with ceaseless increasing demands for palm oil. Optimizing plant architecture to increase radiation interception efficiency could be an option for enhancing potential crop production. Most oil palms grown in the world are Deli *dura* × AVROS *pisifera* crosses displaying large phenotypic variations due to genetic segregation. The objective of this study was to analyse and model oil palm architecture taking into account genetic variability. Data were collected in Sumatra, Indonesia, on 5 progenies (total of 60 palms), to describe the aerial architecture from the leaflet to crown scales. Allometric relationships (using linear and non-linear functions) were applied to model these traits according to ontogenetic gradients and leaf position within the canopy. Results pointed out contrasting architectural traits among genotypes, especially for the leaf insertion angle, leaf length and leaflet shape. Mean values of the simulated architectural traits were compared with field measurements to evaluate the quality of the modelling approach. The allometric relationships, parameterized for different genotypes, were then implemented in the AMAPstudio software to generate 3D mock-ups to estimate integrative traits (such as crown dimensions) that were not directly modelled in the allometric-based model. Forthcoming works will be dedicated to the analysis of the impact of the different architectural characteristics on plant light interception using sensitivity analysis methods in order to identify some key architectural traits that could be considered in breeding programs.

Keywords: plant architecture, *Elaeis guineensis*, genetic variability, 3D reconstruction

INTRODUCTION

Oil palm (*Elaeis guineensis*) is the most important oil crop in the world with an annual production of 47.5 million of ton. The majority of cultivated oil palm in the world comes from Deli *dura* × AVROS *pisifera* crosses. Genetic materials used by breeders are mainly progenies, which correspond to populations of full sib families, obtained from a unique bunch pollinated by the same male inflorescence. Progenies may display large phenotypic variations because of genetic segregation (Jacquemard, 2011). This variability can be observed in terms of yield, plant functioning and plant architecture.

Oil palm architecture follows the Corner model, which is characterized by a mono-axial shoot that produces phytomers in regular succession (Halle and Oldeman, 1970). The phytomer consists of a node to which a leaf and a male or female inflorescence (when abortion does not occur) are attached (Henry, 1958). The crown represents 30 to 45 leaves and each leaf is composed of a petiole and a rachis that bears leaflets. Before the adult phase (i.e., when all the organs reach their final potential size), leaf size increases with plant age. At young stages, these ontogenetic gradients related to leaf size are directly observable according to the topological position of the leaf on the stem (leaf rank).

Computational reconstruction of plant architecture requires modelling the geometry and the topological relationships of all plant components. Various methodologies have been used to reconstruct 3D canopy structures such as digitizing (Sinoquet et al., 1997),

simulation models (Pallas et al., 2013 on oil palm) or other modelling approaches based on local measurements of organ geometry (Louarn et al., 2008). The first method is the most precise but time-consuming. As a consequence it cannot be easily used to describe architectural variability from data collection on several genotypes. Thus this study focuses on a methodology established from local measurements that enables the study of architectural traits considering the genotypic variation of these traits. The present study aimed at simulating the architectural variability of oil palm, and illustrates the use of allometric relationships to capture the main determinants of oil palm aerial architecture and its variability; thus deciphering genetic and non-genetic determinants of the oil palm architecture.

MATERIAL AND METHOD

Model description and calibration

The strategy used to develop the model was based on the following steps: 1) define the variables needed to reconstruct 3D structure; 2) model each variable through allometric relationships to take into account their evolution within the canopy structure; 3) assess progeny and individual effects and calibrate consequences of model parameters; 4) assess model reconstruction comparing integrative traits measured in the field with those simulated using a plant architecture simulator built under the AMAP Studio platform (Griffon and de Coligny, 2014).

Data were collected in 2014 on 12 individuals of 5 different progenies (DA1, DL7, DS, DU, DY4) of African and Indonesian origins in a field trial of SMART Research Institute (SMARTRI, Smart Tbk.) located in Palembang (South Sumatra province, Indonesia). Palms were planted in 2010 and had not yet reached their adult phase when measured. Measurements were performed on stems (stem height and stem basis diameter), leaves (petiole length, rachis length, rachis angles, number of leaflets) and leaflets (lengths, width and insertion angles on rachis). To account for ontogenetic gradients with plant age, the number of leaves emitted since planting (*LeafNb*) was recorded and used as an explanatory variable of organ size (rachis length). Rachis length was then used as an explanatory variable of other plant component dimensions. Finer geometrical traits such as rachis angles were modelled as a function of leaf rank, a variable accounting for the topological position of leaves on the stem (rank 1 was associated with the last leaf emitted and fully open at the tip of the stem). At the leaf scale, variations in leaflet geometry (length, width) were considered based on their position along the rachis. Ten leaflets per leaf were sampled at regular intervals along the rachis and a fine description of their dimensions and shape was performed to estimate individual leaflet area (Talliez and Ballo Koffi, 1992).

The studied variables were modelled using allometric relationships with parameters associated with geometrical properties. Model selection was performed through a likelihood ratio test, to compare function adjustments between progenies. The test was based on a Chi-squared test (χ^2) on nested models (null model, progeny model) which enabled assessment of which model was the most relevant for each variable (null or progeny model). Linear and non-linear functions (polynomial, logistic and exponential) were adjusted to the data collected for each progeny with the nlme package of the R software (R Development Core Team) (equations presented in Figure 1). Each allometric relationship obtained with this methodology was evaluated for consistent fit with the collected data using root mean square errors (RMSE) and bias.

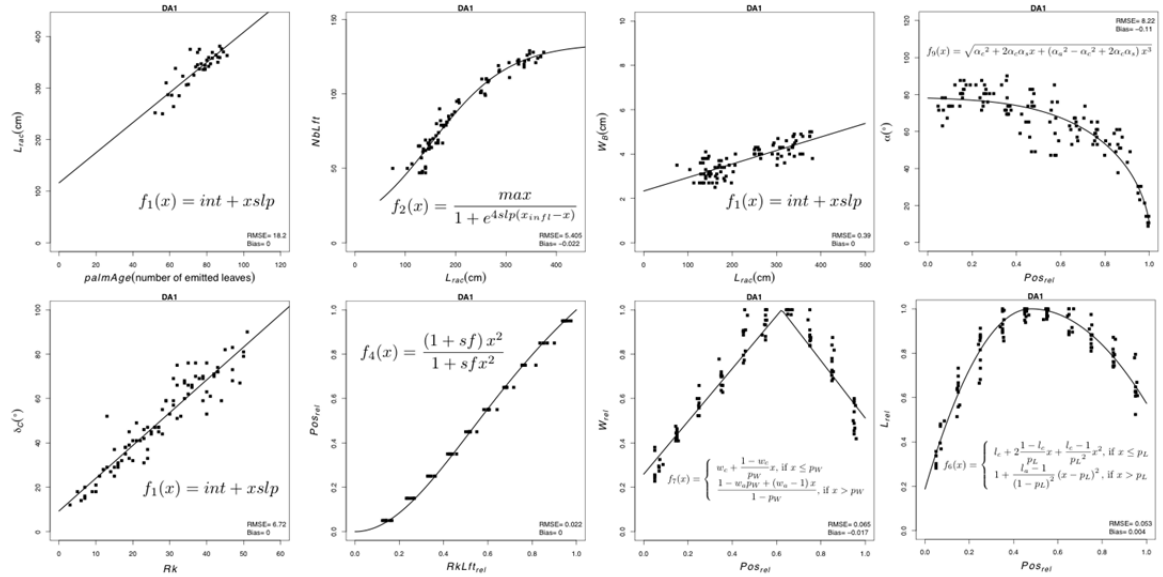

Figure 1. Example of the allometric relationships used in the modelling approach. Data observed on 6 plants (points) and function adjustments (lines) are represented for one progeny (DA1) (*Lrac*: rachis length, *NbLft*: number of leaflets per leaf, L_B: leaflet length at B point (B point is a point of reference on rachis), δ_c: declination at C point (transition point between petiole and rachis), *Rk*: leaf rank, Rk_{Lft}: leaflet rank, Pos_{rel}: relative position on rachis, L_{rel}: leaflet length relatively to the longest on rachis, W_{rel}: leaflet maximum width relatively to the largest leaflet on rachis).

Model simulation and validation

The established allometric relationships were implemented in a dedicated plant simulator (Vpalm) in the AMAPstudio software (Griffon and de Coligny, 2014). This plant simulator was based on a multi-scale organisation of plant components (stem, leaf and leaflets) with a tree graph (Godin and Caraglio, 1998) and rebuilt the topological structure and organ geometry from a parameter file generated for each progeny.

Although the majority of variables in the model were modelled using allometric relationships directly fitted on observed data, other output variables were modelled combining various allometric relationships and thus could have led to error accumulation. As an example, leaflet area along a rachis was a suitable variable to assess model compliance as it results from the combination of several successively assembled variables (Figure 2). Besides the evaluation of organ size, the development of three-dimensional reconstructions also allowed evaluation of model accuracy based on variables related to geometrical characteristics such as leaf angles and orientation, that were not directly modelled by allometric relationships. For this kind of geometrical variable, the height at the rachis tip (H_A) was selected since it combines variables of plant size (stem height, petiole and rachis length) and leaf angles (leaf insertion angle, leaf curvature and deviation). Height at rachis tip was hence measured on several leaf ranks to better assess the architectural gradients within the leaf crown. The results of the simulation for individual leaf areas along the rachis and H_A were then compared (using RMSE and bias) to observed values on plants used for model calibration of the allometric relationships.

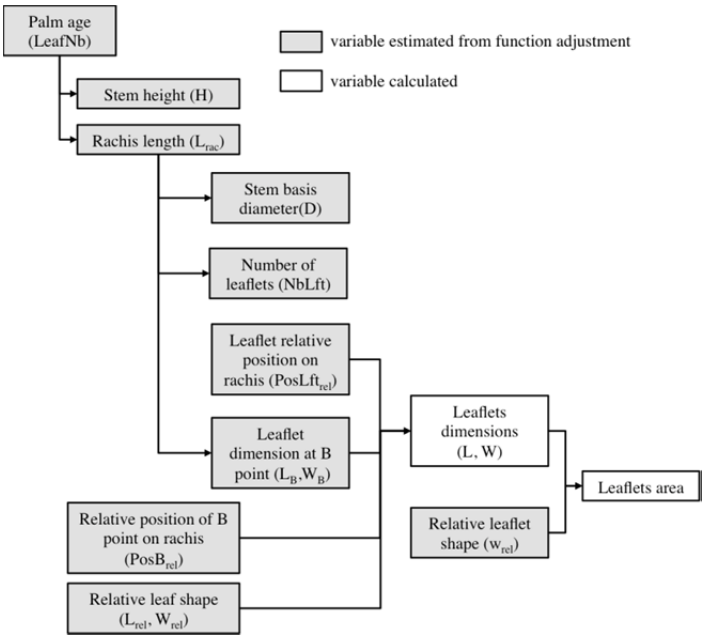

Figure 2. Computation of leaflet area in the allometric based model. Leaflet area was calculated from a succession of allometric relationships allowing the consideration of ontogenetic gradient (through palm tree age) and morphogenetic characteristics of leaflet geometry (through relative leaflet position on rachis).

RESULTS

Model parameterization

The quality of adjustments of the allometric relationships was satisfactory for all the relationships in terms of both RMSE and bias (data only shown for DA1 in Figure 1). Overall, function adjustments showed that the same allometric relationships could be used for all progenies. For rachis length (L_{rac}), the RMSE varied from 12 to 20 cm depending on the progeny (with bias inferior to 1 cm), which was suitable since rachis length was around an average of 350 cm. For leaflet dimensions (L and W), the error varied from 3 to 6 cm in length (mean leaflet length was 60 cm) and 0.3 to 0.4 cm in width (mean leaflet width was 5 cm). For the latter variables the bias was negligible (less than 0.5 cm for length and 0.1 cm for width). Functions associated with finer geometric characteristics such as leaf angles and leaflet insertion angles were also satisfactory (RMSE<6° and |bias| <1° for leaf declination (δ_C) and RMSE<11° and |bias| <0.2° for leaflet axial insertion on rachis (α)).

Results of the models used to fit the allometric relationships highlight a significant effect of progeny for all the variables and revealed the necessity to determine different parameter values for each progeny (Table 1). The values of adjusted parameters gave information about each morphotype related to the progeny. For instance, a quicker increase in rachis length was observed for DY4 ($Lrac_{slp}$=3.36 cm leaf^{-1}) than other progenies ($Lrac_{slp}$ < 3 cm leaf^{-1}). This trend potentially reveals a faster growth rate of this progeny during the first years after planting. Likewise, the greater value of the L_{Bslp} parameter for DA1 (L_{Bslp} = 0.18 cm cm^{-1}) revealed a higher tendency of DA1 to display longer leaflets for a given rachis length. For leaflet width, progeny DU presented larger leaflets (W_{Bslp} = 0.08 cm cm^{-1}), which probably led to less interspace between leaflets than for other progenies. Regarding crown architecture, the declination angle at petiole tip (C point) evolved rapidly for progeny DU compared to the others (δ_{Cslp} = 1.69°/rank against δ_{Cslp} < 1.5°/rank), probably leading to a less erect crown for DU leading to potential differences in canopy light interception. Progeny DA1 and DY4 exhibited lower values of leaflet axial insertion angle (α) and thus reflect less

spread among leaflets along the rachis. Finally, regarding relative leaflet length along the rachis, both progenies DA1 and DY4 had longer leaflets at point C (*lc* is around 0.20 compared to 0.50 for the three other progenies) and a similar position of the longest leaflet on rachis (p_L=0.48).

Table 1. Mean values of parameters associated to allometric relationships.

Predicted variables	Progeny effect	Parameters	DA1	DL7	DS	DU	DY4
Rachis length	***	Intercept	116	97	141	103	92
Lrac=f(LeafNb)		Slope	2.92	2.87	2.32	2.97	3.36
Number of leaflets	***	Max nb of leaflets per leaf	134	124	137	131	130
NbLft=f(Lrac)		Slope factor at inflexion point	0.003	0.005	0.004	0.003	0.005
		Rachis length at inflexion point	151	153	152	153	155
Declination at C point	***	Intercept	9	12	12	10	11
δC=f(Rk)		Slope	1.48	1.44	1.32	1.69	1.48
Posrel f(RkLft)	***	Evolution of inter-leaflets distance along the rachis	2.21	2.32	2.31	2.36	2.40
Leaflet length at point B	***	Intercept	18	26	29	24	29
LB=f(Lrac)		Slope	0.18	0.13	0.14	0.14	0.13
Leaflet width at point B		Intercept	2.6	2.2	2.9	2.2	3.1
WB=f(Lrac)		Slope	0.005	0.006	0.005	0.008	0.004
Leaflet relative length	***	Lrel at point C	0.19	0.04	0.04	0.04	0.21
Lrel=f(Posrel)		Position of the longest leaflet on rachis	0.48	0.43	0.46	0.46	0.48
		Lrel at A point	0.57	0.63	0.48	0.62	0.48
Leaflet relative width	***	Wrel at point C	0.26	0.22	0.19	0.18	0.28
Wrel=f(Posrel)		Position of the largest leaflet on rachis	0.62	0.61	0.60	0.60	0.59
		Wrel at A point	0.51	0.46	0.42	0.52	0.44
Leaflet axial angle	***	Leaflet axial insertion angle at point C	78	90	88	97	82
α=f(Posrel)		Decreasing-factor of axial angle along the rachis	-4	-29	-16	-24	-22
		Leaflet axial insertion angle at point A	10	26	25	22	16

Significance levels of progeny effect correspond to the p-value of the likelihood ratio test (n.s: non significant, *, p<0.05; **, p<0.01; ***, p<0.001).

Assessment of reconstruction model

The model exhibited satisfactory behaviour as simulation results for leaflet area and height at point A were in accordance with observations for all progenies (Figure 3A). Depending on the progeny, RMSE (calculated from 6 individuals per progeny) varied from 13 to 21 cm^2 and bias was less than 8 cm^2. These simulation results showed variations in leaflet area along the rachis for the different progenies. For instance progeny DL7 had smaller leaflet areas compared to the other progenies bearing leaflets that were more than 220 cm^2. Looking at the variability of measurements within the progenies, it is clear that individuals were more homogeneous for the progenies DL7 and DU than for the three others. Indeed, the range of variations of leaflet area was about 100 cm^2 for progenies DA1, DS and DY4, while it hardly reached 50 cm^2 for progenies DL7 and DU.

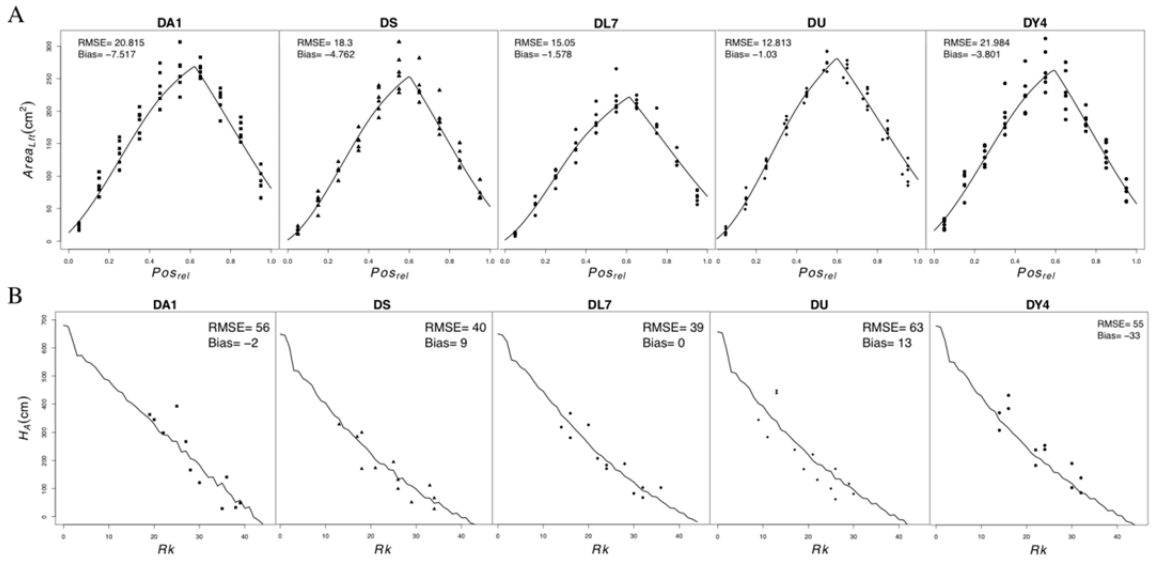

Figure 3. Assessment of model reconstruction. (A) Comparison of observed (points) and simulated (lines) leaflet area ($Area_{Lft}$) along the rachis (Pos_{rel}). (B) Comparison of observed (points) and simulated (lines) heights at rachis tip (H_A) depending on leaf rank (Rk). Results presented in Figure 3B come from 3D mock-ups generated with AMAPStudio.

Figure 3B shows the correspondence between the heights at rachis tip extracted from three-dimensional reconstructions (Figure 4) with actual observations from the field. The results confirm the consistency of model reconstruction since the variable was adequately represented (RMSE<63 cm and |bias|<33 cm). However this indicator only provided information about the quality of leave arrangement in a vertical layer (one dimension).

Figure 4. Example of 3D reconstruction from allometric relationships (progeny DA1, 47 month after planting date). Scale bar = 1 m.

DISCUSSION

Sonohat et al. (2006) showed the benefits of coupling allometric relationships with partial digitizing for building 3D mock-ups and called attention to its potential for describing large numbers of replicates. In the present study, we emphasize the practical application of a method for reconstructing virtual plants entirely based on allometric relationships. This

modelling approach enabled accurate simulation of the architectural variability among progeny of oil palm, considering genotypic characteristics through parameters calibrated from field observations. Statistical analysis performed on the allometric relationships demonstrated that several architectural traits were significantly different among progenies. However high intra-progeny variability was observed with various architectural traits, which has not yet been considered in this modelling approach. Further studies need to be conducted to analyse and integrate variability among individuals belonging to a similar progeny into the model.

The next step of this study will also focus on a methodology to more precisely evaluate model compliance comparing 3D mock-ups with data collected from hemispherical photographs and terrestrial LIDAR. Such a model could be a convenient tool for further studies to understand the relationships between plant structure and functioning (light interception and radiation use efficiency). In the short term, the 3D reconstructions will enable us to perform sensitivity analyses involving architectural parameters in relation to light interception efficiency, as has been done on apple trees (Da Silva et al., 2014). Such studies will aim at identifying key architectural traits to optimize light interception. In addition, others studies could be done using a higher number of progenies grown in contrasting environments to better decompose oil palm architecture plasticity into genetic and environmental effects (Segura et al., 2008). Nevertheless, since the measurements presented in this study were time consuming, the protocol of observations should be simplified. The sensitivity analysis of the impact of architectural traits on light interception could be useful to find relevant variables on which phenotyping could be done on large populations.

ACKNOWLEDGEMENTS

Thanks to SMART Research Institute (SMARTRI, Smart Tbk.) for financial support of this study and to SMARTRI staff for technical assistance with data acquisition.

Literature cited

Da Silva, D., Han, L., Faivre, R., and Costes, E. (2014). Influence of the variation of geometrical and topological traits on light interception efficiency of apple trees: sensitivity analysis and metamodelling for ideotype definition. Ann. Bot. *114* (*4*), 739–752. PubMed http://dx.doi.org/10.1093/aob/mcu034

Godin, C., and Caraglio, Y. (1998). A multiscale model of plant topological structures. J. Theor. Biol. *191* (*1*), 1–46. PubMed http://dx.doi.org/10.1006/jtbi.1997.0561

Griffon, S., and de Coligny, F. (2014). Amapstudio: an editing and simulation software suite for plants architecture modelling. Original research article. Ecol. Modell. *290*, 3–10 http://dx.doi.org/10.1016/j.ecolmodel.2013.10.037.

Halle, F., and Oldeman, R.A.A. (1970). Essai sur l'architecture et la Dynamique de Croissance des Arbres Tropicaux. 6 (Paris, France: Masson et Cie).

Henry, P. (1958). Croissance et développement chez *Elaeis guineensis jacq*. de la germination à la première floraison. Rev. Gen. Bot *66*, 5–34.

Jacquemard, J.-C. (2011). Le Palmier à Huile (Quae, CTA, Presse Agronomiques de Gembloux).

Louarn, G., Lecoeur, J., and Lebon, E. (2008). A three-dimensional statistical reconstruction model of grapevine (*Vitis vinifera*) simulating canopy structure variability within and between cultivar/training system pairs. Ann. Bot. *101* (*8*), 1167–1184. PubMed http://dx.doi.org/10.1093/aob/mcm170

Pallas, B., Clément-Vidal, A., Rebolledo, M.-C., Soulié, J.-C., and Luquet, D. (2013). Using plant growth modeling to analyze C source-sink relations under drought: inter- and intraspecific comparison. Front Plant Sci *4*, 437. PubMed http://dx.doi.org/10.3389/fpls.2013.00437

Segura, V., Cilas, C., and Costes, E. (2008). Dissecting apple tree architecture into genetic, ontogenetic and environmental effects: mixed linear modelling of repeated spatial and temporal measures. New Phytol. *178* (*2*), 302–314. PubMed http://dx.doi.org/10.1111/j.1469-8137.2007.02374.x

Sinoquet, H., Rivet, P., and Godin, C. (1997). Assessment of the three- dimensional architecture of walnut trees using digitising. Silva Fenn. *31* (*3*), 265–273 http://dx.doi.org/10.14214/sf.a8525.

Sonohat, G., Sinoquet, H., Kulandaivelu, V., Combes, D., and Lescourret, F. (2006). Three-dimensional reconstruction of partially 3D-digitized peach tree canopies. Tree Physiol. *26* (*3*), 337–351. PubMed

http://dx.doi.org/10.1093/treephys/26.3.337
Talliez, B., and Ballo Koffi, C. (1992). A method for measuring oil palm leaf area. Oleagineux *47*, 537–545.